Journal of Veterinary Cardiology (2019) **23**, 1—14

Journal of Veterinary Cardiology
ESVC

www.elsevier.com/locate/jvc

Right ventricular function and dyssynchrony measured by echocardiography in dogs with precapillary pulmonary hypertension☆

T. Morita, DVM, PhD [a], K. Nakamura, DVM, PhD [b,*], T. Osuga, DVM, PhD [c], K. Morishita, DVM, PhD [c], N. Sasaki, DVM, PhD [a], H. Ohta, DVM, PhD [a], M. Takiguchi, DVM, PhD [a]

[a] *Laboratory of Veterinary Internal Medicine, Department of Veterinary Clinical Sciences, Graduate School of Veterinary Medicine, Hokkaido University, N18 W9, Sapporo, Hokkaido 060-0818, Japan*
[b] *Organization for Promotion of Tenure Track, University of Miyazaki, 1-1 Gakuenkibanadai-nishi, Miyazaki 889-2192, Japan*
[c] *Veterinary Teaching Hospital, Graduate School of Veterinary Medicine, Hokkaido University, N18 W10, Sapporo, Hokkaido 060-0818, Japan*

Received 30 January 2018; received in revised form 27 November 2018; accepted 21 December 2018

KEYWORDS
Canine;
Speckle-tracking echocardiography;
Strain;
Tei index

Abstract *Introduction:* Assessment of the right ventricular (RV) function by echocardiography is important in dogs with pulmonary hypertension (PH). Few reports are available on RV function and dyssynchrony in dogs, especially in the context of precapillary PH.
Animals: The study included 79 client-owned dogs: 25 dogs with precapillary PH and 54 control dogs.
Methods: Dogs with precapillary PH were prospectively enrolled between December 2013 and February 2017. The echocardiographic indices of RV function, including RV strain and the dyssynchrony index by speckle-tracking echocardiography,

☆ A unique aspect of the Journal of Veterinary Cardiology is the emphasis of additional web-based materials permitting the detailing of procedures and diagnostics. These materials can be viewed (by those readers with subscription access) by going to http://www.sciencedirect.com/science/journal/17602734. The issue to be viewed is clicked and the available PDF and image downloading is available via the Summary Plus link. The supplementary material for a given article appears at the end of the page. To view the material is to go to http://www.doi.org and enter the doi number unique to this paper which is indicated at the end of the manuscript.

* Corresponding author.
E-mail address: kenvet@cc.miyazaki-u.ac.jp (K. Nakamura).

https://doi.org/10.1016/j.jvc.2018.12.005

were measured. Multivariate analysis was used to determine independent predictors of the RV dyssynchrony index.
Results: Dogs with precapillary PH showed RV dilation, hypertrophy and right atrial dilation. Impaired echocardiographic indices of RV function, including RV strain, were observed. In addition, RV dyssynchrony occurred in dogs with precapillary PH. Multivariate analysis revealed that tricuspid regurgitation velocity and RV dilation were independent predictors of the RV dyssynchrony index.
Conclusions: Echocardiographic RV function indices are impaired in dogs with precapillary PH. In addition, RV dilation and elevated systolic pulmonary arterial pressure estimated by echocardiography are associated with RV dyssynchrony.

Abbreviations

Ao	aorta
EI	eccentricity index
FAC	fractional area change
LA	left atrium
LV	left ventricle
MMVD	myxomatous mitral valvular disease
nRVAd	normalized right ventricular end-diastolic area
nRVAs	normalized right ventricular end-systolic area
PA	pulmonary artery
PH	pulmonary hypertension
RA	right atrium
RV	right ventricle
RVAd	right ventricular end-diastolic area
RVAs	right ventricular end-systolic area
RVLS	right ventricular longitudinal strain
RV-SD	standard deviation of systolic shortening time of right ventricle
RV-SD4	standard deviation of systolic shortening time of four mid-basal right ventricular segments
RV-SD6	standard deviation of systolic shortening time of six right ventricular segments
RVWTd	right ventricular wall thickness in diastole
sPAP	systolic pulmonary arterial pressure
SST	systolic shortening time
STE	speckle-tracking echocardiography
S'_{TV}	peak systolic tricuspid annular velocity
TAPSE	tricuspid annulus plane systolic excursion
TR	tricuspid regurgitation

Introduction

Pulmonary hypertension (PH) is a progressive and life-threatening disease characterized by an increase in the pulmonary arterial (PA) pressure and pulmonary vascular resistance leading to right ventricular (RV) pressure overload, dysfunction and death [1]. While PH is classified into five major classes in human medicine [2], a more simplified classification that distinguishes precapillary PH from postcapillary PH is used in dogs [3]. Precapillary PH is defined as PH due to abnormalities of PAs caused by congenital cardiovascular disease, respiratory disease, pulmonary thromboembolism, heartworm disease and hypoxaemia. Conversely, postcapillary PH is caused by the left-sided heart disease, such as myxomatous mitral valvular disease (MMVD).

Both precapillary and postcapillary PH are associated with a poor prognosis in human patients with heart disease [4—8]. In addition, RV function, as evaluated by magnetic resonance imaging, cardiac catheterization and echocardiography has been found to be associated with clinical outcomes and cardiac function in human patients with both precapillary and postcapillary PH [9,10]. Furthermore, RV intraventricular dyssynchrony, which is associated with abnormalities in the timing of RV contraction, has been described in human patients with precapillary PH and has been associated with marked RV dysfunction and clinical worsening [11,12]. Therefore, the assessment of RV function has attracted interest in human medicine.

In the current human guidelines for echocardiographic assessment of the RV size and function, it is recommended to evaluate RV function using multiple echocardiographic indices, including the peak systolic tricuspid annular velocity (S'_{TV}), tricuspid annulus plane systolic excursion (TAPSE), fractional

area change (FAC), RV Tei index and RV longitudinal strain (RVLS) by speckle-tracking echocardiography (STE) [13,14]. In addition, echocardiographic assessment of RV function has recently emerged in dogs [15]. The standard deviation of systolic shortening time of RV (RV-SD), which is an index of RV intraventricular dyssynchrony, has recently been demonstrated to be a good predictor of poorer cardiac function, clinical worsening and prognosis in human patients with precapillary PH [16–18].

Postcapillary PH is a factor indicating poor prognosis in dogs with MMVD [19], and several echocardiographic indices of RV function have been used to assess RV function in dogs with postcapillary PH. Serres et al. [20] reported that S'_{TV} was significantly impaired in dogs with precapillary and postcapillary PH. In contrast, Baron Toaldo et al. [21] showed that S'_{TV} did not change in dogs with postcapillary PH due to MMVD. Tai and Huang [22] reported that TAPSE/aorta (Ao) was similar to controls in dogs with chronic respiratory disease, heartworm disease and MMVD. Conversely, Pariaut et al. [23] showed that TAPSE was significantly decreased in dogs with severe PH due to the left-sided heart disease, heartworm disease and pulmonary disease compared with milder PH and control dogs. Other researchers have reported that the Tei index, as measured by pulsed-wave Doppler, was significantly increased in dogs with precapillary and postcapillary PH [24]. In addition, we have previously reported that the Tei index as measured by dual pulsed-wave Doppler was an independent predictor of cardiac-related mortality within 1 year in MMVD dogs with and without PH [25].

To our knowledge, little is known about changes in multiple echocardiographic indices of RV function, including RVLS derived from STE, in dogs exhibiting exclusively precapillary PH. In addition, no report is currently available on RV dyssynchrony in dogs with PH. The authors hypothesized that RV dysfunction and dyssynchrony would occur in dogs with precapillary PH. The primary objective of this study was to evaluate RV function and RV dyssynchrony by echocardiography in dogs with precapillary PH compared with control dogs. In addition, our secondary objective was to validate factors that influence RV dyssynchrony in dogs with precapillary PH.

Animals, materials and methods

Animals

Client-owned dogs, referred to the Veterinary Teaching Hospital of Hokkaido University between December 2013 and February 2017, were prospectively evaluated. The owner's consent for each dog was obtained before its enrolment in this study. Pulmonary hypertension was defined as a maximum continuous-wave Doppler tricuspid regurgitation (TR) velocity faster than 2.8 m/s or pulmonic insufficiency velocity faster than 2.2 m/s, without pulmonic stenosis [3]. Pulmonic stenosis was excluded when normal blood flow velocity (1.5 m/s) was obtained at the RV outflow tract by Doppler echocardiography. Dogs with the left atrial (LA) dilation (LA to Ao diameter ratio $>$ 1.6) and a high transmitral early diastolic flow velocity ($>$1.0 m/s) were excluded. Dogs of any age and size of breed were included in the present study. To investigate the origin of the PH, radiography was performed in all dogs with PH, and computed tomography examination was performed in dogs suspected of respiratory disease and pulmonary thromboembolism.

Client-owned dogs referred to the Veterinary Teaching Hospital of Hokkaido University between December 2013 and February 2017 with no evidence of cardiovascular disorders were included as control dogs. The purpose for undertaking ultrasonographic evaluation of control dogs was pre-anaesthesia assessment or medical examination. All control dogs were determined to have a normal heart anatomy and myocardial function based on normal findings on complete physical examination, electrocardiography and standard echocardiographic examinations (including B-mode, M-mode, pulsed-wave Doppler and colour flow Doppler imaging). A small thin central TR jet on colour flow Doppler and a faint TR signal on continuous-wave Doppler were defined as trivial TR. Dogs with 'silent regurgitation' across the tricuspid and pulmonic valves were not excluded because this is considered physiological in many healthy dogs [26].

Echocardiographic measurements

Conventional echocardiographic examinations were performed with an ultrasound unit[d] equipped with a 3–6 MHz sector probe[e] by an echocardiographer (K.N.). All dogs were examined without sedation in the left and right lateral recumbent positions. An ECG trace (lead II) was recorded simultaneously. QRS duration was manually measured by ECG trace (lead II).

[d] Artida, Toshiba Medical Systems Corporation, Utsunomiya, Tochigi, Japan.
[e] PST-50BT, Toshiba Medical Systems Corporation, Utsunomiya, Tochigi, Japan.

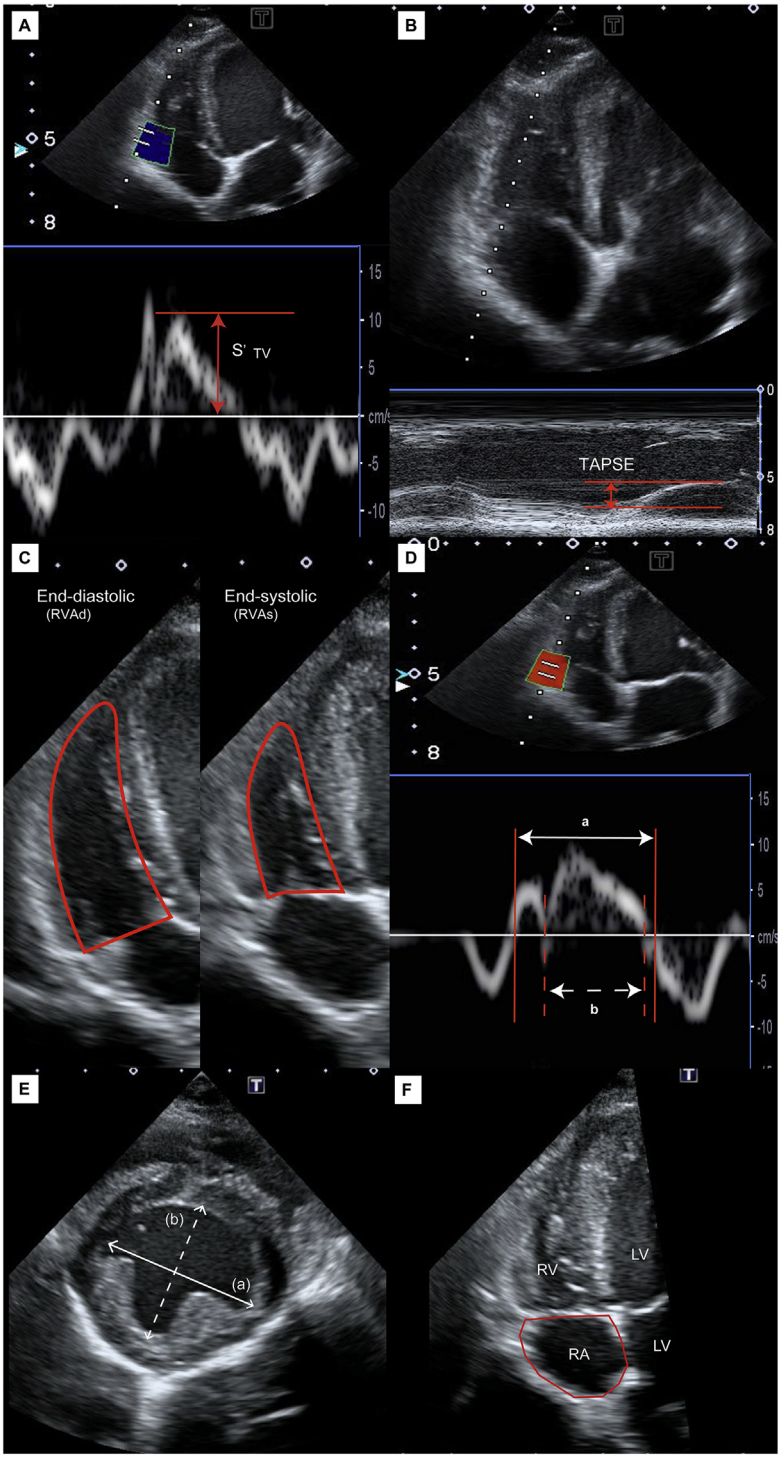

Figure 1 Echocardiographic images illustrating a technique used to measure echocardiographic indices of RV function. (A) The peak systolic tricuspid annular velocity was determined by measuring the maximum velocity during systole using tissue Doppler at the lateral tricuspid annulus from a left apical four-chamber view, (B) tricuspid annulus plane systolic excursion was determined by measuring the amplitude of tricuspid annulus motion during systole using the M-mode from a left apical four-chamber view, (C) fractional area change was calculated from a modified left apical four-chamber view as follows: (RVAd−RVAs)/RVAd × 100%, (D) the Tei index was calculated using tissue Doppler at the lateral tricuspid annulus from a left apical four-chamber view as follows: (a−b)/b, (E) the eccentricity index was calculated with a right parasternal short-axis view as follows: long axis (a)/short axis (b) and (F) the right atrial area was measured by planimetrically tracing end-systole from a modified left apical four-chamber view. RV, right ventricle; RVAd, RV end-diastolic area; RVAs, RV end-systolic area; S'_{TV}, systolic tricuspid annular velocity; TAPSE, tricuspid annular plane systolic excursion; RA, right atrium; LV, left ventricle.

The RV diameter and the RV wall thickness in diastole (RVWTd) were obtained by M-mode echocardiography from a right parasternal short-axis view at the level of the papillary muscles. The RV diameter in diastole was normalized for body weight using the following equations: normalized RV diameter in diastole = RV diameter in diastole/(body weight)$^{0.33}$ [27]. The LA and Ao diameters were obtained from a right parasternal short-axis view at the level of the LA, and the LA/Ao ratio was calculated [28]. The LA to Ao diameter ratio >1.6 was considered indicative of LA dilation [28]. The PA valve annulus diameter was obtained from a right parasternal short-axis view at the level of the PA, and the PA/Ao ratio was calculated [3]. Pulmonary artery to Ao diameter ratio >0.98 was considered indicative of PA dilation [3]. Measurements of transmitral early diastolic flow velocity were obtained by pulsed-wave Doppler from a left apical four-chamber view. The acceleration time to the ejection time of the PA ratio was measured from a left cranial parasternal short-axis view [3]. The peak TR velocity was measured using the echocardiographic view that provided the highest velocity. The systolic pulmonary arterial pressure (sPAP) was estimated by calculating the peak TR gradient using the simplified Bernoulli equation: sPAP = 4 × peak TR^2 + right atrial (RA) pressure. The RA pressure was estimated to be 5 mmHg when there was no evidence of RA dilation, 10 mmHg if there was RA dilation and no evidence of right-sided congestive heart failure and 15 mmHg if there was evidence of the right-sided congestive heart failure [29].

The S'$_{TV}$ was obtained by tissue Doppler at the RV free wall tricuspid annulus from a left apical four-chamber view (Fig. 1). Tricuspid annulus plane systolic excursion was generated from the M-mode recording with a cursor over the RV free wall tricuspid annulus from a left apical four-chamber view (Fig. 1). The TAPSE was normalized to the body weight as follows: nTAPSE = TAPSE/(body weight)$^{0.33}$ [27]. The RV end-diastolic area (RVAd) and RV end-systolic area (RVAs) were obtained from a modified left apical four-chamber view optimized for the right heart by tracing the RV endocardium in systole and diastole via the RV free wall to the apex and back to the annulus, along the septum. To obtain a modified left apical four-chamber view, the transducer was rotated until the maximal plane of the RV basal diameter was obtained. The RV should not be foreshortened, and visualization of the left ventricular (LV) outflow tract should be avoided [13,15]. The FAC was calculated as (RVAd−RVAs)/RVAd × 100% (Fig. 1). Right ventricular end-diastolic area and RVAs were normalized according to the following equation [30]: normalized RVAd (nRVAd) and RVAds (nRVAs) = RVAd and RVAs/body surface area. The RV Tei index was calculated as the sum of the isovolumic contraction time and isovolumic relaxation time divided by ejection time. The ejection time was defined as the S'$_{TV}$ duration, and the sum of the isovolumic time was derived by subtracting the S'$_{TV}$ duration from the time interval between the end of the late diastolic tricuspid annulus velocity and the onset of the early diastolic tricuspid annulus velocity on the basis of tissue Doppler recordings (Fig. 1) [13]. To evaluate LV compression, the eccentricity index (EI) was measured as the ratio of the long-axis to short-axis diameters of the LV from a right parasternal short-axis view at the level of papillary muscle obtained at end-systole (Sys EI) and end-diastole (Dia EI) (Fig. 1) [22]. The RA area was measured by planimetrically tracing end-systole from the lateral aspect of the tricuspid annulus to the septal aspect, excluding the inferior and superior vena cava and RA appendage, from a modified left apical four-chamber view optimized for the right heart [31] (Fig. 1). The RA area was normalized according to the following equation [31]: normalized RA area = RA area/body surface area.

Right ventricular longitudinal strain and RV-SD analysis by STE

The RVLS and RV-SD were analysed using conventional echocardiographic greyscale from a modified left apical four-chamber view optimized for the right heart [13,15] with a frame rate of >200 frames/s. To optimize the frame rate, the imaging sector was narrowed, and the depth was reduced. Three consecutive cardiac cycles were acquired and digitally stored, and the images were analysed using offline software.[f] The region of interest was obtained by manually tracing the RV endocardial border at the level of the septum and free wall at end-diastole and adjusted to incorporate the entire RV wall myocardial thickness. The RV free wall and septum were divided into three segments each (basal, middle and apical) and further divided into inner and outer layers. The RVLS is a measurement of myocardial tissue deformation and defined as the change in length of region of interest relative to its original

[f] 2D Wall Motion Tracking, Toshiba Medical Systems Corporation, Utsunomiya, Tochigi, Japan.

length. The RVLS is expressed as a negative percentage, and negative strain values describe shortening of the region of interest [32]. The RVLS was obtained for the six RV segments at the maximum peak of the software-generated strain curves of the inner layer.

Global RVLS was automatically calculated by averaging peak longitudinal strain values observed in six segments (basal, middle and apical segments of RV free wall and septum), and the free wall RVLS and septal RVLS were calculated by averaging peak longitudinal strain values of the three segments (basal, middle and apical segments) of the RV free wall or septum. In addition, the global RVLS was also calculated by averaging the peak longitudinal strain values observed in four mid-basal segments of the RV, and the free wall RVLS and septal RVLS were calculated by averaging peak longitudinal strain values observed in two mid-basal segments of the RV free wall or septum (Fig. 2). The systolic shortening time (SST) was calculated from the QRS onset to the maximum longitudinal strain of each of the RV segments. The RV intraventricular dyssynchrony was derived by calculating the standard deviation of the SST of six segments (RV-SD6) or standard deviation of the SST of four mid-basal segments (RV-SD4) using offline software[f] (Fig. 2), and each RV-SD was corrected for the RR interval according to Bazett's formula: Corrected RV-SD = RV-SD/$\sqrt{}$RR interval [33].

Statistical analysis

The normality of the distribution of the data was tested with a Shapiro–Wilk test. Continuous data are reported as median (interquartile range), and categorical data are reported as counts (proportions). The comparison of group characteristics and echocardiographic indices were performed using Wilcoxon rank-sum tests for continuous variables and with the Fisher's exact test for categorical variables. The correlation between the TR velocity and echocardiographic indices of RV function; RV-SD and QRS duration, TR velocity, sPAP estimated by echocardiography and RV and RA morphologic variables; RV-SD and other echocardiographic indices of RV function were evaluated by Spearman's rank correlation coefficient analysis.

To assess the independent predictor of RV-SD4, TR velocity, normalized RV diameter in diastole, nRVAd, nRVAs, Sys EI, Dia EI, RVWTd, normalized RA area and QRS duration were included in multiple linear regression analysis with forward stepwise selection and Akaike information criterion.

All statistical analyses were performed using computer software.[g] A p-value of less than 0.05 was considered significant.

Results

Clinical characteristics in dogs with precapillary PH

Among the 79 dogs included in this study, 25 dogs had precapillary PH and 54 were control dogs. Dogs with precapillary PH belonged to 13 different breeds, with Welsh corgi being the most frequently represented (n = 5), followed by Miniature dachshund and Chihuahua (n = 3 each); Shih tzu, Yorkshire terrier, West Highland white terrier and mixed breeds (n = 2 each) and a Shetland sheepdog, Miniature schnauzer, American cocker spaniel, Cavalier King Charles spaniel, Toy poodle and Shiba inu (n = 1 each). Eleven of 25 dogs with precapillary PH had respiratory disease with concurrent radiographic or computed tomographic evidence of pulmonary alveolar or interstitial infiltrates, five dogs had congenital heart disease (patent ductus arteriosus, ventricular septal defect and atrial septal defect), one dog had acute pulmonary thromboembolism with concurrent computed tomographic evidence of PA occlusion, one dog had suspected pulmonary thromboembolism with concurrent echocardiographic evidence of a large thrombus inside the RV and one dog had heartworm disease. In six dogs, the left heart disease was excluded, although the cause of PH could not be determined.

Conventional echocardiographic variables in dogs with precapillary PH and control dogs

Conventional echocardiographic characteristics of the two groups are summarized in Table 1. On echocardiography, 22 dogs with precapillary PH had TR, and eight dogs had pulmonic insufficiency. Seventeen dogs with precapillary PH had main PA dilation (PA/Ao diameter ratio > 0.98), and 16 dogs showed septal flattening. In dogs with precapillary PH, the age, heart rate, QRS duration, TR velocity and sPAP estimated by echocardiography were significantly higher than those in control dogs. Dogs with precapillary PH showed RV and PA dilation, RV hypertrophy and RA

[g] JMP version 8.0, SAS Institute Inc., Cary, NC, U.S.A.

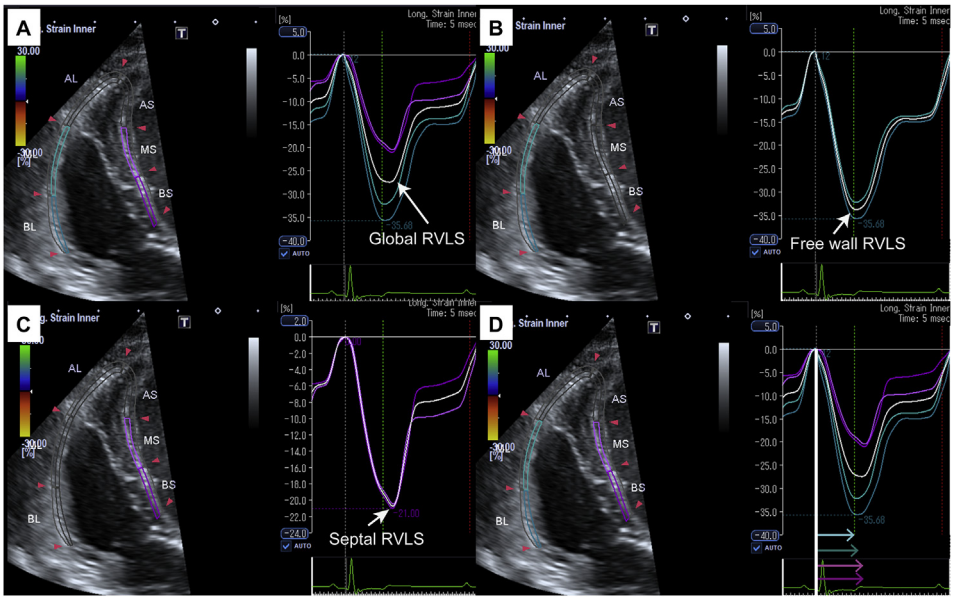

Figure 2 Echocardiographic images illustrating a technique used to measure STE indices. The RV free wall and septum were automatically divided into three segments (apical, middle and basal), respectively. (A) Global RVLS was calculated by averaging peak longitudinal strain values in four mid-basal segments of RV with a left modified apical four-chamber view, (B) the free wall RVLS was calculated by averaging peak longitudinal strain values in two mid-basal free wall segments of the RV, (C) septal RVLS was calculated by averaging peak longitudinal strain values in two mid-basal septal segments of the RV and (D) the standard deviation of SST of four mid-basal RV segments was calculated and corrected for the R—R interval (Bazett's formula). The coloured arrows indicate each segmental SST. STE, speckle-tracking echocardiography; RV, right ventricle; RVLS, RV longitudinal strain; AL, apical lateral free wall; AS, apical septum; BL, basal lateral free wall; BS, basal septum, ML, middle lateral free wall; MS, middle lateral septum; SST, systolic shortening time. White lines indicate averaging peak longitudinal strain values.

dilation based on echocardiography findings. Although several RV function indices, such as the nTAPSE, FAC and the Tei index, were significantly impaired, the other RV function indices, including the S'_{TV} and TAPSE, were not altered in dogs with precapillary PH.

Speckle-tracking echocardiographic variables in dogs with precapillary PH and control dogs

Three dogs with precapillary PH had inadequate images of the apical segment for STE. In contrast, segmental RVLS using four mid-basal segments and RV-SD4 was obtained in all dogs with precapillary PH.

Dogs with precapillary PH showed a decreased global, free wall and septal RVLS, longer free wall SST and increased RV-SD6 and RV-SD4 (Fig. 3 and Table 1).

Correlation analysis

The correlations between TR velocity and echocardiographic indices of RV function are summarized in Table 2. In dogs with precapillary PH, FAC, the Tei index, global RVLS, septal RVLS, RV-SD6 and RV-SD4 were moderately correlated with the TR velocity.

The correlations between RV-SD and RV morphologic and electrical variables, estimated sPAP by echocardiography and RA area are summarized in Table 3. The RV-SD6 was moderately correlated with nRVAd, nRVAs, Sys EI, Dia EI and sPAP but was not correlated with RVWTd or QRS duration in dogs with precapillary PH. The RV-SD4 was moderately correlated with nRVAd, nRVAs, Sys EI, Dia EI, sPAP, and normalized RA area but was not correlated with RVWTd or QRS duration.

The correlations between RV-SD and the other echocardiographic indices of RV function are summarized in Table 4. The correlation analysis revealed that RV-SD6 was moderately correlated with global RVLS, free wall RVLS, septal RVLS, FAC and the Tei index, and RV-SD4 was moderately correlated with global RVLS, septal RVLS, FAC and the Tei index.

Multiple linear regression analysis

Multiple linear regression analysis revealed that TR velocity and nRVAs were independent predictors of the RV-SD6 (TR velocity, $\beta = 0.37$, p=0.012; RVAs,

Table 1 Comparison of clinical and echocardiographic variables in 25 dogs with precapillary pulmonary hypertension and 54 control dogs.

Variables	Precapillary PH	n	Control	n	*p*
Male/female	12/13	25	28/26	54	.44
Age (year)[a]	12 (9–13)	24	9 (8–10)	54	.005
Body weight (kg)	6.9 (3.7–10.1)	25	5.3 (3.3–8.7)	54	.31
Heart rate (bpm)[a]	136 (110–147)	25	92 (80–111)	54	<.001
Mean BP (mmHg)	115 (100–135)	16	109 (97–119)	40	.10
QRS duration (msec)[a]	60 (56–62)	25	57 (53–59)	54	.03
Right heart failure[a]	4 (16.7%)		0 (0%)		.01
Medication					
Sildenafil	4 (16.0%)		0 (0%)		
Beraprost sodium	3 (12.0%)		0 (0%)		
Prednisolone	3 (12.0%)		0 (0%)		
Echocardiography					
TR velocity (m/s)[a]	3.7 (3.1–4.5)	22	2.3 (2.2–2.5)	10	<.001
Systolic PAP (mmHg)[a]	58.9 (44.5–82.3)	22	26.1 (22.9–33.6)	10	<.001
RA pressure					
5 (mmHg)	12 (48.0%)		54 (100%)		
10 (mmHg)	9 (36.0%)		0 (0%)		
15 (mmHg)	4 (16.0%)		0 (0%)		
PR velocity (m/s)	3.0 (2.4–3.5)	8	1.8 (1.8–1.8)	1	.18
LA/Ao	1.37 (1.25–1.43)	25	1.39 (1.27–1.50)	54	.43
RV and RA morphologic variables					
nRVIDD[a]	0.60 (0.46–0.88)	24	0.41 (0.36–0.48)	54	<.001
nRVAd (cm^2/m^2)[a]	18.5 (15.6–28.2)	25	11.3 (8.9–13.7)	54	<.001
nRVAs (cm^2/m^2)[a]	11.9 (9.5–19.9)	25	6.8 (4.9–8.4)	54	<.001
Sys EI[a]	1.35 (1.21–1.50)	24	0.95 (0.91–0.98)	50	<.001
Dia EI[a]	1.45 (1.14–1.64)	25	1.02 (0.98–1.05)	50	<.001
PA/Ao[a]	1.15 (0.99–1.24)	22	0.87 (0.80–0.93)	33	<.001
RVWTd (mm)[a]	4.8 (3.5–6.9)	23	3.0 (2.5–3.7)	54	<.001
nRAA (cm^2/m^2)[a]	8.9 (7.5–13.3)	25	5.6 (4.5–7.1)	54	<.001
RV function index					
S'_{TV} (cm/s)	10.5 (8.4–12.6)	24	9.7 (8.4–12.8)	53	.90
TAPSE (mm)	8.1 (7.2–10.7)	25	9.2 (7.9–11.4)	52	.10
nTAPSE[a]	0.45 (0.35–0.58)	25	0.53 (0.46–0.62)	52	.04
FAC (%)[a]	32.9 (24.9–37.2)	25	42.4 (35.5–47.6)	54	<.001
Tei index[a]	0.70 (0.56–0.83)	23	0.52 (0.47–0.55)	53	<.001
AT/ET[a]	0.28 (0.22–0.34)	25	0.38 (0.35–0.41)	54	<.001
STE variables (6-segment)					
Global RVLS × −1 (%)[a]	12.0 (7.7–14.3)	22	17.1 (15.8–18.8)	54	<.001
Free wall RVLS × −1 (%)[a]	12.2 (8.5–16.1)	22	18.4 (17.1–20.7)	54	<.001
Septal RVLS × −1 (%)[a]	8.6 (6.3–12.2)	22	15.6 (13.9–16.5)	54	<.001
Free wall SST (msec)	215 (186–251)	22	192 (178–214)	54	.05
Septal SST (msec)	206 (184–242)	22	190 (176–218)	54	.10
RV-SD6 (msec)[a]	27.2 (16.3–70.8)	22	16.6 (10.0–20.3)	54	<.001
STE variables (4-segment)					
Global RVLS × −1 (%)[a]	12.6 (9.1–16.6)	25	19.6 (16.9–21.5)	54	<.001
Free wall RVLS × −1 (%)[a]	13.3 (11.1–16.9)	25	21.3 (19.0–23.7)	54	<.001
Septal RVLS × −1 (%)[a]	10.3 (7.9–14.8)	25	17.0 (15.1–18.8)	54	<.001
Free wall SST (msec)[a]	217 (190–244)	25	190 (181–214)	54	.03

(*continued on next page*)

Table 1 (*continued*)

Variables	Precapillary PH	n	Control	n	*p*
Septal SST (msec)	199 (174–235)	25	189 (174–215)	54	.52
RV-SD4 (msec)[a]	24.1 (18.4–68.8)	25	12.7 (7.4–17.7)	54	<.001

AT/ET, acceleration time to ejection time of pulmonary artery flow ratio; BP, blood pressure; BSA, body surface area; Dia EI, eccentricity index at end-diastole; FAC, fractional area change; LA/Ao, left atrium to aorta diameter ratio; nRAA, normalized RA area; nRVAd, normalized RV end-diastolic area; nRVAs, normalized RV end-systolic area; nRVIDD, normalized RV diameter in diastole; nTAPSE, normalized tricuspid annular plane systolic excursion; PA/Ao, pulmonary artery to aorta diameter ratio; PAP, pulmonary arterial pressure; PH, pulmonary hypertension; PR, pulmonic regurgitation; RA, right atrium; RVLS, RV longitudinal strain; RV-SD4, standard deviation of systolic shortening time of 4 mid-basal segments of RV; RV-SD6, standard deviation of systolic shortening time of 6 RV segments; RVWTd, RV wall thickness in diastole; SST, systolic shortening time; S'_{TV}, systolic tricuspid annular velocity; STE, speckle-tracking echocardiography; Sys EI, eccentricity index at end-systole; TAPSE, tricuspid annular plane systolic excursion; TR, tricuspid regurgitation; RV, right ventricle.

Data are expressed as the median (interquartile range) for continuous data or number (percentage) for categorical data.

[a] Values between the two groups differed significantly ($p<0.05$).

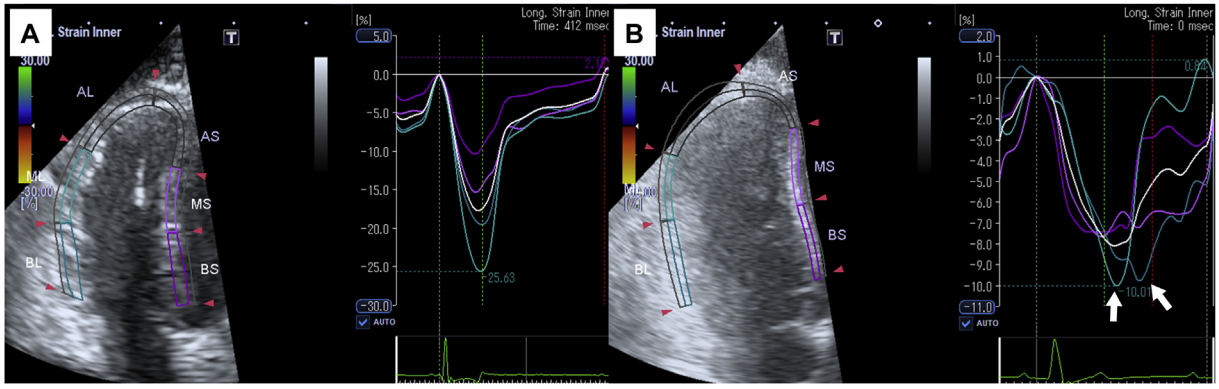

Figure 3 Representative images of STE from a 2-year-old castrated male Chihuahua (control dogs) (A) and a 12-year-old spayed female American cocker spaniel with precapillary PH due to acute pulmonary thromboembolism (B). (A) Global RVLS was −18.4%, free wall RVLS was −21.6%, septal RVLS was −15.1%, and RV-SD4 was 16.0 msec. (B) Global RVLS was −6.7%, free wall RVLS was −7.5%, septal RVLS was −6.7%, and RV-SD4 was 101.8 msec. Free wall segments (ML and BL) were delayed compared with septal segments (MS and BS). STE, speckle-tracking echocardiography; RV, right ventricle; RVLS, RV longitudinal strain; PH, pulmonary hypertension; RV-SD4, standard deviation of systolic shortening time of four mid-basal segments of RV; BL, basal lateral free wall; ML, middle lateral free wall; MS, middle lateral septum; BS, basal septum.

$\beta = 0.57$, $p<0.001$). Tricuspid regurgitation velocity and nRVAs were independent predictors of the RV-SD4 (TR velocity, $\beta = 0.42$, $p=0.003$; RVAs, $\beta = 0.51$, $p<0.001$).

Discussion

The main finding of this study is that echocardiographic indices of RV function, including FAC, the Tei index and RVLS derived from STE, are impaired in dogs with precapillary PH. In addition, these dogs showed severe RV dyssynchrony assessed by RV-SD6, and RV-SD4 derived from the STE and RV dyssynchrony was associated with RV dilation and an elevated sPAP.

To our knowledge, the present study is the first to describe RVLS values derived from STE in dogs with precapillary PH. The present findings are comparable to previous reports in human patients with precapillary PH [34–36]. Speckle-tracking echocardiography is a novel quantitative method for assessment of the regional and global myocardial deformation based on greyscale B-mode images. This method can be used to evaluate the ventricular performance without being influenced by angle dependence or geometric assumptions [37]. In human patients with precapillary PH, RVLS is negatively correlated with PA pressure and pulmonary vascular resistance [34,38,39] and has been reported to be a good predictor of a poor outcome, reduced cardiac function and clinical

Table 2 Correlation analysis of tricuspid regurgitation velocity and echocardiographic indices of the right ventricular function in 25 dogs with precapillary pulmonary hypertension.

Variables	*r*	*p*
S'_{TV} (cm/s)	−0.32	.16
TAPSE (mm)	−0.12	.60
nTAPSE	−0.02	.94
FAC (%)[a]	−0.49	.022
Tei index[a]	−0.55	.013
6-segment global RVLS × - 1 (%)[a]	−0.54	.012
6-segment free wall RVLS × - 1 (%)	−0.34	.13
6-segment septal RVLS × - 1 (%)[a]	−0.61	.003
RV-SD6 (msec)[a]	0.71	<.001
4-segment global RVLS × - 1 (%)[a]	−0.59	.004
4-segment free wall RVLS × - 1 (%)	−0.31	.16
4-segment septal RVLS × - 1 (%)[a]	−0.60	.003
RV-SD4 (msec)[a]	−0.71	<.001

S'_{TV}, systolic tricuspid annular velocity; nTAPSE, normalized tricuspid annular plane systolic excursion; TAPSE, tricuspid annular plane systolic excursion; FAC, fractional area change; RVLS, RV longitudinal strain; RV, right ventricle; RV-SD6, standard deviation of systolic shortening time of 6 RV segments; RV-SD4, standard deviation of systolic shortening time of 4 mid-basal segments of RV.
[a] $p < 0.05$.

Table 3 Correlation analysis of the standard deviation of systolic shortening time of four mid-basal right ventricular segments and QRS duration, tricuspid regurgitation velocity, systolic pulmonary arterial pressure and right ventricle and atrium morphologic variables in 25 dogs with precapillary pulmonary hypertension.

Variables	RV-SD6		RV-SD4	
	r	*p*	*R*	*p*
QRS duration (msec)	−0.03	.89	0.02	.93
TR velocity (m/sec)	0.70[a]	<.001	0.71[a]	<.001
Systolic PAP	0.68[a]	<.001	0.76[a]	<.001
nRVIDD	0.27	.22	0.36	.082
nRVAd (cm^2/m^2)	0.59[a]	.003	0.63[a]	<.001
nRVAs (cm^2/m^2)	0.65[a]	<.001	0.71[a]	<.001
Sys EI	0.44[a]	.035	0.44[a]	.030
Dia EI	0.53[a]	.008	0.50[a]	.011
RVWTd	0.33	.13	0.30	.17
nRAA	0.39	.060	0.60[a]	<.001

RV, right ventricle; RV-SD6, standard deviation of systolic shortening time of 6 RV segments; RV-SD4, standard deviation of systolic shortening time of 4 mid-basal segments of RV; TR, tricuspid regurgitation; PAP, pulmonary arterial pressure; nRVIDD, normalized RV diameter in diastole; nRVAd, normalized RV end-diastolic area; nRVAs, normalized RV end-systolic area; Sys EI, eccentricity index at end-systole; Dia EI, eccentricity index at end-diastole; RVWTd, RV wall thickness in diastole; nRAA, normalized RA area.
[a] $p < 0.05$.

Table 4 Correlation analysis of the standard deviation of systolic shortening time of four mid-basal right ventricular segments and the other echocardiographic indices of the right ventricular function in 25 dogs with precapillary pulmonary hypertension.

Variables	RV-SD6		RV-SD4	
	r	*p*	*r*	*p*
S'_{TV} (cm/s)	0.03	.90	−0.04	.85
TAPSE (mm)	−0.03	.90	−0.05	.83
nTAPSE	−0.04	.84	−0.03	.90
FAC (%)	−0.49[a]	.015	−0.53[a]	.002
Tei index	−0.58[a]	.004	−0.55[a]	.007
6-segment global RVLS × - 1 (%)	−0.52[a]	.010		
6-segment free wall RVLS × - 1 (%)	−0.43[a]	.036		
6-segment septal RVLS × - 1 (%)	−0.44[a]	.034		
4-segment global RVLS × - 1 (%)			−0.59[a]	.002
4-segment free wall RVLS × - 1 (%)			−0.37	.068
4-segment septal RVLS × - 1 (%)			−0.51[a]	.010

RV, right ventricle; RV-SD6, standard deviation of systolic shortening time of 6 RV segments; RV-SD4, standard deviation of systolic shortening time of 4 mid-basal segments of RV; S'_{TV}, systolic tricuspid annular velocity; nTAPSE, normalized tricuspid annular plane systolic excursion; TAPSE, tricuspid annular plane systolic excursion; FAC, fractional area change; RVLS, RV longitudinal strain.
[a] $p < 0.05$.

worsening [34—36]. Further studies are necessary to clarify whether RVLS is useful for assessing haemodynamic changes and prognosis in dogs with precapillary PH.

This study provides the first description of RV dyssynchrony in dogs with precapillary PH. We applied both a six-segment and four-segment RV model to assess RV dyssynchrony. Some dogs had inadequate images of apical segments in the present study. The reason for the inadequate images of apical segments might be related to RV dilation or tachypnoea. In several previous human studies, a four-segment RV model was applied in patients with precapillary PH [16,17]. Conversely, one previous human study demonstrated that RV-SD6 was a stronger prognostic index than RV-SD4 in patients with precapillary PH [18]. Therefore, further studies are needed to determine which dyssynchrony index is superior for assessing RV dyssynchrony.

In the present study, RV dyssynchrony determined by RV-SD6 and RV-SD4 occurred in dogs with precapillary PH, and these dogs had a longer free

wall SST and similar septal SST compared with control dogs. These results agree with those of human studies by Marcus et al. [11] and Kalogeropoulos et al. [12], which demonstrated that free wall systolic delay assessed by magnetic resonance imaging and STE occurred in patients with precapillary PH. This indicates that RV dyssynchrony in dogs with precapillary PH is also caused by free wall systolic delay.

In human patients with precapillary PH, RV dilation (RVAd and Dia EI), elevated afterload and a longer QRS duration contributed to RV dyssynchrony [11,16–18]. Our findings are partially consistent with human studies. The results of the present study demonstrate that there is a significant correlation between RV-SD and RV dilation (nRVAs, nRVAd, Sys EI and Dia EI) and sPAP estimated by echocardiography. In addition, nRVAs and TR velocity were independent predictors of RV-SD6 and RV-SD4 on multiple linear regression analysis. While the longer QRS duration has been reported to contribute to RV dyssynchrony in human patients with precapillary PH [16], it was not related to RV-SD6 and RV-SD4 in the present study. The reason for this disagreement may be the difference in the proportion of subjects with a wide QRS duration, heterogeneity of dogs with precapillary PH and small sample size. The present findings suggest that RV dilation and elevated afterload contribute to RV dyssynchrony in dogs with precapillary PH.

It has been reported that afterload elevation induces LV dyssynchrony even in normal subjects [40]. Additionally, we previously reported that mild RV pressure overload without RV dilation caused RV dyssynchrony in dog models of acute mild RV pressure overload [41]. Furthermore, RV dilation and elevated afterload increase RV wall stress according to Laplace's law. In human patients with precapillary PH, increased RV wall stress was associated with RV dyssynchrony based on magnetic resonance imaging [11]. The combination of these factors contributes to RV dyssynchrony.

In the present study, S'_{TV} and TAPSE were not altered in dogs with precapillary PH. In contrast, FAC and the Tei index were significantly impaired. Previous human studies reported that these echocardiographic indices significantly decreased and were good predictors of a poor prognosis in human patients with precapillary PH [34,36,38,42]. Furthermore, in dogs with precapillary and postcapillary PH, S'_{TV} and TAPSE were decreased compared with control dogs [20,23]. One reason for this difference may be the effect of body weight. Our group and Visser et al. [44] previously reported that the S'_{TV}, TAPSE and the Tei index were positively correlated, while FAC was negatively correlated with body weight [43]. In fact, nTAPSE was significantly decreased in dogs with precapillary PH in the present study. Another reason may be an angle-dependence and regional analysis of tricuspid annulus of S'_{TV} and TAPSE. Given these findings, the FAC and the Tei index might be more sensitive to changes in RV haemodynamics and function than the S'_{TV} and TAPSE.

The severity of PH is assessed by Doppler-estimated sPAP in dogs [3,23,45]. However, the estimation of sPAP by echocardiography has technical limitations. Estimated sPAP cannot be measured in dogs without a TR. Conversely, echocardiographic indices of RV function may be applied even in dogs without TR. In addition, some echocardiographic indices of RV function, such as FAC, the Tei index and RVLS, were significantly correlated with the estimated sPAP in the present study. Therefore, these indices are useful for assessing the severity of PH. However, these echocardiographic indices may be affected by volume overload, such as TR and pulmonic insufficiency. Indeed, we determined that echocardiographic indices of RV function were enhanced by acute volume overload in healthy Beagles [46]. In the present study, there was no difference in echocardiographic indices between control dogs with TR and those without TR (data not shown). A potential explanation for this result may be the severity of TR in control dogs. In the present study, the severity of TR was mild in all control dogs. Further studies are needed to clarify the effect of TR on echocardiographic indices of RV function in dogs with PH.

There remain several limitations in the present study. First, the number of dogs with precapillary PH was small. Therefore, the study had limited power for detecting differences between groups. Second, the aetiology causing precapillary PH was heterogeneous. Different effects due to acute or chronic RV pressure overload on RV function have been reported in human patients [47]. However, the effects of different underlying conditions causing PH (e.g. acute or chronic) on echocardiographic indices of RV function could not be assessed in the present study. Third, no gold standard assessment of RV haemodynamics, such as the right heart catheterisation, was evaluated in the present study. Therefore, the relationship between changes in echocardiographic indices and haemodynamic variables in dogs with precapillary PH cannot be ascertained. Fourth, dogs with precapillary PH were diagnosed by echocardiography, and the PA wedge pressure was not measured by

cardiac catheterisation in the present study. Thus, the possibility of postcapillary PH could not be completely excluded. Fifth, some dogs were being treated with sildenafil and beraprost sodium. While these drugs possess the potential for affecting RV function owing to reducing RV afterload, the effects of these drugs on RV function have not been clarified in dogs. Further studies are needed to reveal the effects of medication on RV function. Sixth, while we evaluated the intraobserver and interobserver repeatability of RVLS and RV-SD6 in healthy Beagles [43], those of RVLS and RV-SD4 in dogs with precapillary PH were not clarified. Finally, RV strain and RV-SD4 were measured using software for LV strain as software specific for RV strain analysis has not yet been developed.

Conclusions

In conclusion, some echocardiographic indices of RV function were significantly impaired, and RV synchronicity was lost in dogs with precapillary PH. The echocardiographic indices of RV dyssynchrony may represent a novel diagnostic approach for detecting PH and might be helpful for elucidating the pathophysiology of RV dysfunction in dogs with PH.

Conflict of interest statement

The authors do not have any conflicts of interest to disclose.

Funding

This study was partially supported by a Grant-in-Aid for Scientific Research from the Japanese Society for the Promotion of Science (No. 16K18800).

Supplementary data

Supplementary data to this article can be found online at https://doi.org/10.1016/j.jvc.2018.12.005.

References

[1] Chin KM, Rubin LJ. Pulmonary arterial hypertension. J Am Coll Cardiol 2008;51:1527—38.
[2] Simonneau G, Gatzoulis MA, Adatia I, Celermajer D, Denton C, Ghofrani A, Gomez Sanchez MA, Krishna Kumar R, Landzberg M, Machado RF, Olschewski H, Robbins IM, Souza R. Updated clinical classification of pulmonary hypertension. J Am Coll Cardiol 2013;62:D34—41.
[3] Kellihan HB, Stepien RL. Pulmonary hypertension in dogs: diagnosis and therapy. Vet Clin North Am Small Anim Pract 2010;40:623—41.
[4] Lowe BS, Therrien J, Ionescu-Ittu R, Pilote L, Martucci G, Marelli AJ. Diagnosis of pulmonary hypertension in the congenital heart disease adult population: impact on outcomes. J Am Coll Cardiol 2011;58:538—46.
[5] Andersen CU, Mellemkjar S, Hilberg O, Nielsen-Kudsk JE, Simonsen U, Bendstrup E. Pulmonary hypertension in interstitial lung disease: prevalence, prognosis and 6 min walk test. Respir Med 2012;106:875—82.
[6] Grigioni F, Potena L, Galiè N, Fallani F, Bigliardi M, Coccolo F, Magnani G, Manes A, Barbieri A, Fucili A, Magelli C, Branzi A. Prognostic implications of serial assessments of pulmonary hypertension in severe chronic heart failure. J Heart Lung Transplant 2006;25:1241—6.
[7] Miller WL, Grill DE, Borlaug BA. Clinical features, hemodynamics, and outcomes of pulmonary hypertension due to chronic heart failure with reduced ejection fraction: pulmonary hypertension and heart failure. J Am Coll Cardiol Hear Fail 2013;1:290—9.
[8] Tatebe S, Fukumoto Y, Sugimura K, Miyamichi-Yamamoto S, Aoki T, Miura Y, Nochioka K, Satoh K, Shimokawa H. Clinical significance of reactive postcapillary pulmonary hypertension in patients with left heart disease. Circ J 2012;76:1235—44.
[9] Van De Veerdonk MC, Kind T, Marcus JT, Mauritz G-J, Heymans MW, Bogaard H-J, Boonstra A, Marques KMJ, Westerhof N, Vonk-Noordegraaf A. Progressive right ventricular dysfunction in patients with pulmonary arterial hypertension responding to therapy. J Am Coll Cardiol 2011;58:2511—9.
[10] Brittain EL, Pugh ME, Wheeler LA, Robbins IM, Loyd JE, Newman JH, Larkin EK, Austin ED, Hemnes AR. Shorter survival in familial versus idiopathic pulmonary arterial hypertension is associated with hemodynamic markers of impaired right ventricular function. Pulm Circ 2013;3:589—98.
[11] Marcus JT, Gan CT, Zwanenburg JJ, Boonstra A, Allaart CP, Götte MJ, Vonk-Noordegraaf A. Interventricular mechanical asynchrony in pulmonary arterial hypertension: left-to-right delay in peak shortening is related to right ventricular overload and left ventricular underfilling. J Am Coll Cardiol 2008;51:750—7.
[12] Kalogeropoulos AP, Georgiopoulou VV, Howell S, Pernetz M-A, Fisher MR, Lerakis S, Martin RP. Evaluation of right intraventricular dyssynchrony by two-dimensional strain echocardiography in patients with pulmonary arterial hypertension. J Am Soc Echocardiogr 2008;21:1028—34.
[13] Rudski LG, Lai WW, Afilalo J, Hua L, Handschumacher MD, Chandrasekaran K, Solomon SD, Louie EK, Schiller NB. Guidelines for the echocardiographic assessment of the right heart in adults:A report from the American society of echocardiography. J Am Soc Echocardiogr 2010;23:685—713.
[14] Lang RM, Badano LP, Mor-Avi V, Afilalo J, Armstrong A, Ernande L, Flachskampf FA, Foster E, Goldstein SA, Kuznetsova T, Lancellotti P, Muraru D, Picard MH, Rietzschel ER, Rudski L, Spencer KT, Tsang W, Voigt J-U. Recommendations for cardiac chamber quantification by

echocardiography in adults: an update from the American society of echocardiography and the European association of cardiovascular imaging. J Am Soc Echocardiogr 2015;28: 1—39.
[15] Visser LC. Right ventricular function: imaging techniques. Vet Clin North Am Small Anim Pract 2017;47:989—1003.
[16] Badagliacca R, Reali M, Poscia R, Pezzuto B, Papa S, Mezzapesa M, Nocioni M, Valli G, Giannetta E, Sciomer S, Iacoboni C, Fedele F, Vizza CD. Right intraventricular dyssynchrony in idiopathic, heritable, and anorexigen-induced pulmonary arterial hypertension: clinical impact and reversibility. J Am Coll Cardiol Imaging 2015;8: 642—52.
[17] Badagliacca R, Poscia R, Pezzuto B, Papa S, Gambardella C, Francone M, Mezzapesa M, Nocioni M, Nona A, Rosati R, Sciomer S, Fedele F, Dario Vizza C. Right ventricular dyssynchrony in idiopathic pulmonary arterial hypertension: determinants and impact on pump function. J Heart Lung Transplant 2015;34:381—9.
[18] Murata M, Tsugu T, Kawakami T, Kataoka M, Minakata Y, Endo J, Tsuruta H, Itabashi Y, Maekawa Y, Fukuda K. Right ventricular dyssynchrony predicts clinical outcomes in patients with pulmonary hypertension. Int J Cardiol 2017; 228:912—8.
[19] Borgarelli M, Abbott J, Braz-Ruivo L, Chiavegato D, Crosara S, Lamb K, Ljungvall I, Poggi M, Santilli RA, Häggström J. Prevalence and prognostic importance of pulmonary hypertension in dogs with myxomatous mitral valve disease. J Vet Intern Med 2015;29:569—74.
[20] Serres F, Chetboul V, Gouni V, Tissier R, Sampedrano CC, Pouchelon J-L. Diagnostic value of echo-Doppler and tissue Doppler imaging in dogs with pulmonary arterial hypertension. J Vet Intern Med 2007;21:1280—9.
[21] Baron Toaldo M, Poser H, Menciotti G, Battaia S, Contiero B, Cipone M, Diana A, Mazzotta E, Guglielmini C. Utility of tissue Doppler imaging in the echocardiographic evaluation of left and right ventricular function in dogs with myxomatous mitral valve disease with or without pulmonary hypertension. J Vet Intern Med 2016;30: 697—705.
[22] Tai TC, Huang HP. Echocardiographic assessment of right heart indices in dogs with elevated pulmonary artery pressure associated with chronic respiratory disorders, heartworm disease, and chronic degenerative mitral valvular disease. Vet Med (Praha) 2013;58:613—20.
[23] Pariaut R, Saelinger C, Strickland KN, Beaufrère H, Reynolds CA, Vila J. Tricuspid annular plane systolic excursion (TAPSE) in dogs: reference values and impact of pulmonary hypertension. J Vet Intern Med 2012;26:1148—54.
[24] Teshima K, Asano K, Iwanaga K, Koie H, Uechi M, Kato Y, Kutara K, Edamura K, Hasegawa A, Tanaka S. Evaluation of right ventricular Tei index (index of myocardial performance) in healthy dogs and dogs with tricuspid regurgitation. J Vet Med Sci 2006;68:1307—13.
[25] Nakamura K, Morita T, Osuga T, Morishita K, Sasaki N, Ohta H, Takiguchi M. Prognostic value of right ventricular Tei Index in dogs with myxomatous mitral valvular heart disease. J Vet Intern Med 2016;30:69—75.
[26] Bonagura JD, Miller MW. Doppler Echocardiography II. Color Doppler imaging. Vet Clin North Am Small Anim Pract 1998;28:1361—89.
[27] Tidholm A, Höglund K, Häggström J, Ljungvall I. Diagnostic value of selected echocardiographic variables to identify pulmonary hypertension in dogs with myxomatous mitral valve disease. J Vet Intern Med 2015;29:1510—7.
[28] Hansson K, Häggström J, Kvart C, Lord P. Left atrial to aortic root indices using two-dimensional and M-mode echocardiography in cavalier King Charles spaniels with and without left atrial enlargement. Vet Radiol Ultrasound 2002;43:568—75.
[29] Kittleson M, Kienle R. Pulmonary arterial and systemic arterial hypertension. In: Kittleson M, Kienle R, editors. Small Animal Cardiovasular Medicine. Saint Louis: Mosby; 1998. p. 433—49.
[30] D'Oronzio U, Senn O, Biaggi P, Gruner C, Jenni R, Tanner FC, Greutmann M. Right heart assessment by echocardiography: gender and body size matters. J Am Soc Echocardiogr 2012;25:1251—8.
[31] Vezzosi T, Domenech O, Iacona M, Marchesotti F, Zini E, Venco L, Tognetti R. Echocardiographic evaluation of the right atrial area index in dogs with pulmonary hypertension. J Vet Intern Med 2018;32:42—7.
[32] Pirat B, McCulloch ML, Zoghbi WA. Evaluation of global and regional right ventricular systolic function in patients with pulmonary hypertension using a novel speckle tracking method. Am J Cardiol 2006;98:699—704.
[33] Bazett HC. An analysis of the time-relations of electrocardiograms. Heart 1920;7:353—70.
[34] Fukuda Y, Tanaka H, Sugiyama D, Ryo K, Onishi T, Fukuya H, Nogami M, Ohno Y, Emoto N, Kawai H, Hirata K-I. Utility of right ventricular free wall speckle-tracking strain for evaluation of right ventricular performance in patients with pulmonary hypertension. J Am Soc Echocardiogr 2011; 24:1101—8.
[35] Fine NM, Chen L, Bastiansen PM, Frantz RP, Pellikka PA, Oh JK, Kane GC. Outcome prediction by quantitative right ventricular function assessment in 575 subjects evaluated for pulmonary hypertension. Circ Cardiovasc Imaging 2013; 6:711—21.
[36] Motoji Y, Tanaka H, Fukuda Y, Ryo K, Emoto N, Kawai H, Hirata K. Efficacy of right ventricular free-wall longitudinal speckle-tracking strain for predicting long-term outcome in patients with pulmonary hypertension. Circ J 2013;77: 756—63.
[37] Mondillo S, Galderisi M, Mele D, Cameli M, Lomoriello VS, Zacà V, Ballo P, D'Andrea A, Muraru D, Losi M, Agricola E, D'Errico A, Buralli S, Sciomer S, Nistri S, Badano L. Speckle-tracking echocardiography: a new technique for assessing myocardial function. J Ultrasound Med 2011;30:71—83.
[38] Li Y, Xie M, Wang X, Lu Q, Fu M. Right ventricular regional and global systolic function is diminished in patients with pulmonary arterial hypertension: a 2-dimensional ultrasound speckle tracking echocardiography study. Int J Cardiovasc Imaging 2013;29:545—51.
[39] Puwanant S, Park M, Popovic ZB, Wilson Tang WH, Farha S, George D, Sharp J, Puntawangkoon J, Loyd JE, Erzurum SC, Thomas JD. Ventricular geometry, strain, and rotational mechanics in pulmonary hypertension. Circulation 2010; 121:259—66.
[40] Miyoshi H, Oishi Y, Mizuguchi Y, Ishimoto T, Nagase N, Yamada H, Mishiro Y, Oki T. Left ventricular systolic asynchrony is induced even in the normal heart during increases in afterload: a study with angiotensin II stress pulsed tissue Doppler imaging. J Echocardiogr 2007;5: 41—7.
[41] Morita T, Nakamura K, Osuga T, Yokoyama N, Morishita K, Sasaki N, Ohta H, Takiguchi M. Changes in right ventricular function assessed by echocardiography in dog models of mild RV pressure overload. Echocardiography 2017;34: 1040—9.
[42] Forfia PR, Fisher MR, Mathai SC, Housten-Harris T, Hemnes AR, Borlaug BA, Chamera E, Corretti MC, Champion HC, Abraham TP, Girgis RE, Hassoun PM. Tricuspid annular displacement predicts survival in

pulmonary hypertension. Am J Respir Crit Care Med 2006; 174:1034—41.
[43] Morita T, Nakamura K, Osuga T, Yokoyama N, Nisa K, Morishita K, Sasaki N, Ohta H, Takiguchi M. The repeatability and characteristics of right ventricular longitudinal strain imaging by speckle tracking echocardiography in healthy dogs. J Vet Cardiol 2017;19:351—62.
[44] Visser LC, Scansen BA, Schober KE, Bonagura JD. Echocardiographic assessment of right ventricular systolic function in conscious healthy dogs: repeatability and reference intervals. J Vet Cardiol 2015;17:83—96.
[45] Poser H, Berlanda M, Monacolli M, Contiero B, Coltro A, Guglielmini C. Tricuspid annular plane systolic excursion in dogs with myxomatous mitral valve disease with and without pulmonary hypertension. J Vet Cardiol 2017;19: 228—39.
[46] Morita T, Nakamura K, Osuga T, Yokoyama N, Morishita K, Sasaki N, Ohta H, Takiguchi M. Effect of acute volume overload on echocardiographic indices of right ventricular function and dyssynchrony assessed by use of speckle tracking echocardiography in healthy dogs. Am J Vet Res 2019;80:51—60.
[47] Ichikawa K, Dohi K, Sugiura E, Sugimoto T, Takamura T, Ogihara Y, Nakajima H, Onishi K, Yamada N, Nakamura M, Nobori T, Ito M. Ventricular function and dyssynchrony quantified by speckle-tracking echocardiography in patients with acute and chronic right ventricular pressure overload. J Am Soc Echocardiogr 2013;26:483—92.